GDCh Research Article Angewandte International Edition Chemie www.angewandte.org

How to cite: *Angew. Chem. Int. Ed.* **2025**, e202513159
doi.org/10.1002/anie.202513159

Metallocages

Low Symmetry Cage Complexes Formed by Metalation of Symmetric Hexa-Cationic Organic Cages

Rosemary J. Goodwin, Annie L. Colebatch, and Nicholas G. White**

Abstract: Most metal organic cages are assembled through metal–ligand coordination, resulting in cages where the metal ions are part of the cage architecture, and thus have limited reactivity. There are only a handful of metal organic cages produced by metalation of a pre-synthesised organic cage. In this work, we show that hexa-cationic hydrazone cages coordinate a range of transition metal ions upon deprotonation to give cage complexes with metal ions oriented towards the cage cavity. Remarkably, a cage with ethyl solubilising groups gives the expected three-fold symmetric metallocage, cages with alkoxy solubilising groups give low-symmetry zinc metallocages, and a cage without a solubilising group switches between high and low symmetry conformations depending on solvent. These low symmetry arrangements persist on the NMR timescale at temperatures as high as 360 K and in the presence of a wide range of anions.

Introduction

Self-assembled cages are discrete 3D structures that can typically be prepared relatively easily, and contain internal cavities that have the potential to replicate the substrate binding pockets of enzymes.[1] However, almost all biological systems have low symmetry binding clefts. This allows them to bind guests with very high specificity, and the precise arrangement of components allows them to carry out complex chemical tasks. In contrast, the overwhelming majority of self–assembled cages are high symmetry species, meaning that high fidelity guest binding is limited to guests with similarly high symmetry. As a result, there has recently been a significant focus on finding ways to prepare low symmetry self–assembled cages both for selective recognition of low symmetry guests and because of the more structurally complex architectures that result.

Most of this attention has focused on metal organic cages assembled through coordination bonds, and significant success has been realised in this area (Figure 1a).[2–4] A combination of steric clashes between certain ligands and favourable interactions between others has been used to disfavour homoleptic cage assembly and favour heteroleptic structures,[5–7] while an alternative approach uses complementarity between ligands with different geometries to drive systems to low symmetry products.[8–19] Significant success has been achieved and remarkably cages containing four different ligands such as $Pd_2L^aL^bL^cL^d$ systems have been prepared.[20–22]

Attempts to prepare low symmetry self–assembled organic cages have not reached the level of complexity seen with metallocages, but some success has been achieved. This has largely focused on either imine cages,[23–25] or "semi-stepwise" syntheses where imine cages are synthesised and then "locked" by further chemical modification.[26–28] Far more success has been realised using stepwise syntheses,[29–32] but cages made in this manner typically require lengthy multi-step syntheses resulting in low product yields.

An alternative approach to low symmetry cages would be to synthesise a high symmetry organic cage through a self–assembly strategy, and then metalate this cage in such a manner that the symmetry of the resulting species is reduced (Figure 1b).[33] As far as we are aware, such an approach combining high symmetry cage components and metal ions to give a lower symmetry architecture would be unprecedented. As well as removing the need to synthesise multiple different ligands, it would have the advantage that introducing metal ions into the cage after cage synthesis would potentially give coordinatively unsaturated metal ions that may be useful for sensing or catalysis applications (in contrast to typical metal organic cages where the metal ions are coordinatively saturated, and displacing the ligand causes degradation of the cage, Figure 1a). While there have been some reports of the post-synthetic metalation of organic cages,[34–42] we do not know of any that result in formation of a low symmetry species.

We recently reported a general route to a small family of three-fold symmetric organic hydrazone cages that were prepared on 7–14 g scale in two steps from commercially available starting materials.[43] One of these, ^{Et}**cage**$^{6+}$

[*] Dr. R. J. Goodwin, Dr. A. L. Colebatch, A/Prof. N. G. White
Research School of Chemistry, Australian National University, Canberra, ACT 2601, Australia
E-mail: annie.colebatch@anu.edu.au
nicholas.white@anu.edu.au

URLs: www.colebatchlab.com, www.nwhitegroup.com

Additional supporting information can be found online in the Supporting Information section

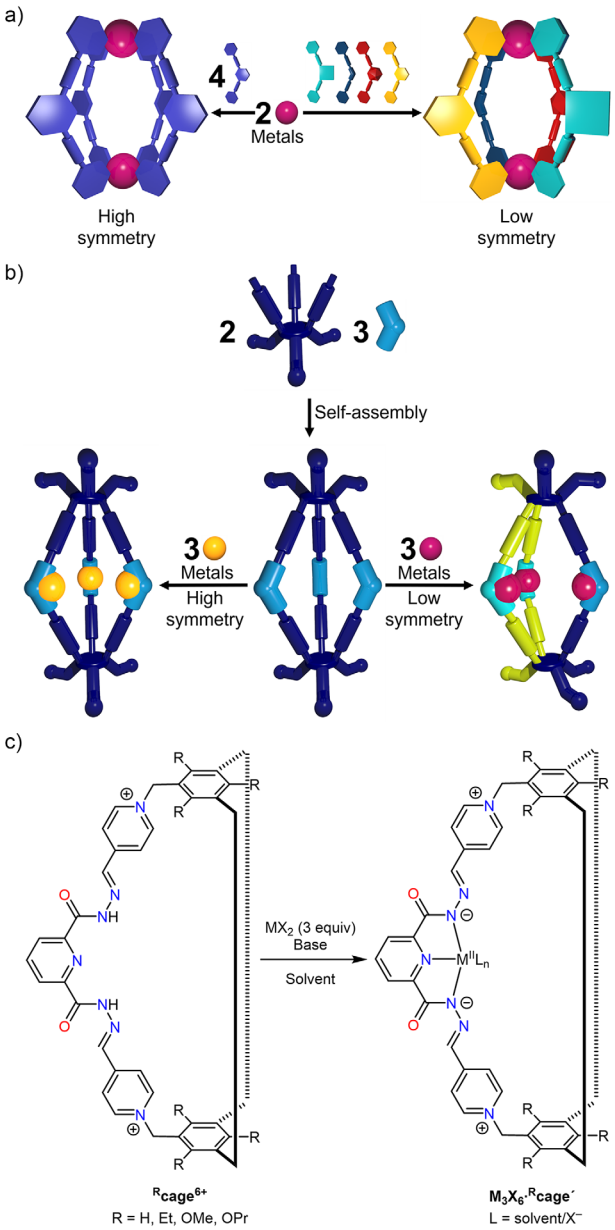

Figure 1. a) Schematic showing high symmetry and low symmetry metallocages formed from self–assembly of coordinatively-saturated architectural metal ions with ligands; b) schematic showing self–assembly of a high symmetry organic cage and its post-synthetic metalation leading to either high symmetry or low symmetry metallocages; c) diagram showing structure of cages used in this work and their metal complexes (in each case only one arm of the cage is shown for clarity with the others represented by bold and dotted lines).

(Figure 1c), contains three pyridyl-2,6-diamide motifs and X-ray crystal structures of ^{Et}**cage**·**Br$_6$** and ^{Et}**cage**·**(PF$_6$)$_6$** revealed a wide cavity with the pyridyl-2,6-diamide groups pointing towards this central cage cavity. These motifs are known to act as dianionic chelating NNN pincer ligands upon deprotonation,[36,44,45] and often give complexes with interesting reactivity[46–51] or sensing[52] properties. In this work, we report our studies on metalation of ^{Et}**cage^{6+}** and related cages containing alkoxy solubilising groups instead of ethyl groups.[53–55] We demonstrate that metalation of ^{Et}**cage^{6+}** results in trimetallic cage complexes with the expected three-fold symmetry, while metalation of alkoxy-substituted cages results in unexpected formation of persistent low-symmetry metallocages.

Results and Discussion

Synthesis of ^{Et}cage·Br$_6$ and ^{OPr}cage·Br$_6$

Ethyl-substituted cage ^{Et}**cage**·**Br$_6$** was synthesised on an 8 g scale in 81% yield over two steps from commercially-available materials, with the cage precipitating from the reaction in pure form, as described previously.[43] The solubility of this cage and its metal complexes are not particularly high, and so we prepared the propoxy-substituted cage ^{OPr}**cage**·**Br$_6$** by an analogous synthetic pathway, although we were unable to find conditions where this cage precipitated from the reaction. Instead, we precipitated ^{OPr}**cage**·**(BF$_4$)$_6$** from the aqueous reaction mixture using $NaBF_4$ and then conducted an anion exchange reaction to give the desired bromide salt of the cage (see Supporting Information Section 1). Despite these challenges, we were still able to obtain clean ^{OPr}**cage**·**Br$_6$** in 61% overall yield from known[56] 1,3,5-tripropoxy-2,4,6-tris(bromomethyl)benzene. The BF_4^- and Br^- salts of the new cage were fully characterised by ESI mass spectrometry, ^{1}H, ^{13}C{^{1}H}, ^{19}F and DOSY NMR spectroscopies (calculated solvodynamic radii = 14.7 and 15.4 Å for BF_4^- and Br^- salts, respectively, these values are consistent with the crystal structures of complexes of this cage, see later).

Complexation of ^{Et}Cage·Br$_6$ With First-row Transition Metal Ions Gives Three-fold Symmetric Complexes

The cages contain potential NNN tridentate binding motifs, which would be expected to complex transition metals upon deprotonation. However, they also contain cationic regions due to the presence of six pyridinium groups, so we were unsure if this would hinder binding to metal ions. We initially studied the metalation of ^{Et}**cage**·**Br$_6$** with first row transition metals ($CoBr_2$, $NiBr_2$, $CuBr_2$, and $ZnBr_2$)[57] in the presence of base by UV–vis spectroscopy and mass spectrometry. In all cases, both techniques were consistent with the formation of **M$_3$Br$_6$**·^{Et}**cage′** species where **cage′** is the zwitterionic form of the cage where all six NH groups have been deprotonated (see Supporting Information Sections 6 and 7).[58]

More detailed NMR studies on metal binding were conducted using diamagnetic $ZnBr_2$ and $[PdBr_2(NCCH_3)_2]$ (see later). Adding NEt_3 to a solution of ^{Et}**cage**·**Br$_6$** in DMSO-d_6 resulted in a colour change from yellow to orange, but ^{1}H NMR spectroscopy indicated little deprotonation in the absence of a metal ion. Addition of $ZnBr_2$ resulted in a colour change to yellow and formation of a three-fold symmetric species with peak positions consistent with deprotonation of all amide-like N–H groups to give **Zn$_3$Br$_6$**·^{Et}**cage′** (Figure 2a).

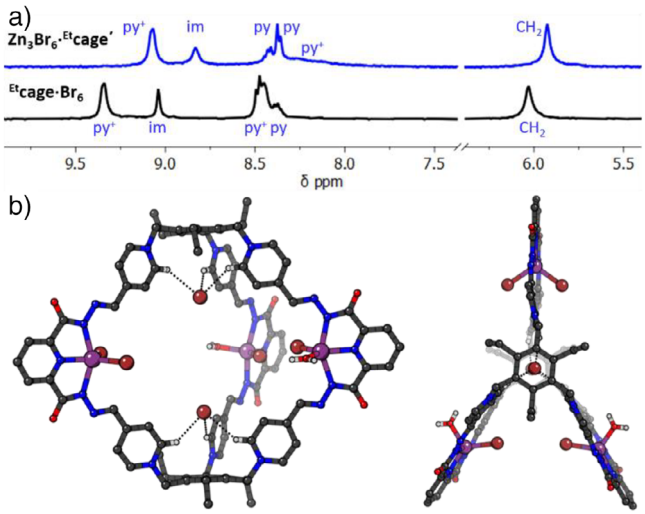

Figure 2. Complexation of $ZnBr_2$ to ^{Et}**cage·Br$_6$**: a) partial ^{1}H NMR spectra of ^{Et}**cage·Br$_6$**, and **Zn$_3$Br$_6$·^{Et}cage′** (2.0 mM in DMSO-d$_6$, 298 K, 400 MHz); b) two views of the X-ray crystal structure of **Zn$_3$Br$_6$·^{Et}cage′** (dotted lines indicate H-bonding interactions shorter than the sum of the van der Waals radii[61] of H and Br), PLATON-SQUEEZE[62] was used to remove ill-defined solvent molecules in the cage cavity.

Slight peak broadening is observed at room temperature, but the peaks sharpen upon heating (Figure S78).

We were able to obtain single crystals of several cage complexes suitable for X-ray diffraction studies. In the interests of brevity, the crystal structure of **Zn$_3$Br$_6$·^{Et}cage′** is shown in Figure 2b, while the structures of the related complexes **Zn$_3$(OAc)$_6$·^{Et}cage′** (obtained by the reaction of ^{Et}**cage·(OAc)$_6$**, NaOH and $Zn(OAc)_2{\cdot}2H_2O$) and **Cu$_3$Br$_6$·^{Et}cage′**, are provided in the Supporting Information (Figures S146 and S149). The crystal structure of **Zn$_3$Br$_6$·^{Et}cage′** contains three five-coordinate zinc(II) ions with geometries somewhere between square pyramidal and trigonal bipyramidal (Addison/Reedijk[59] parameters τ_5 = 0.38 and 0.39 for the two crystallographically-independent Zn(II) ions). The coordination bonds with the central pyridyl donors are shorter than those to the deprotonated amide donors, as is commonly observed for these kind of pincer motifs (Zn–$N_{pyridine}$: 2.054(5), 2.059(7) Å, Zn–N_{amide} = 2.184(6) – 2.216(5) Å), see Supporting Information Section 9 for Cambridge Structural Database[60] (CSD) analysis of related complexes.

We have previously observed that the tris-pyridinium "caps" of the cage interact strongly with bromide anions,[43] so it is perhaps unsurprising that two Br^- anions occupy these locations, forming charge-assisted hydrogen bonds with pyridinium C–H groups. The remaining four bromides are coordinated to Zn(II) centres, with one metal centre binding two bromides, and the remainder each coordinating one bromide anion and a water molecule. The overall architectures of **Cu$_3$Br$_6$·^{Et}cage′** and **Zn$_3$(OAc)$_6$·^{Et}cage′** are very similar to that of **Zn$_3$Br$_6$·^{Et}cage′**, both having three metal ions with geometries intermediate between square pyramidal and trigonal bipyramidal, and with all three "arms" of the cage well-separated from one another.

Complexation of ^{OPr}Cage·Br$_6$ With ZnBr$_2$ Gives Low Symmetry Complexes

We next studied the metalation of propoxy-substituted ^{OPr}**cage·Br$_6$** with first row transition metals ($CoBr_2$, $NiBr_2$, $CuBr_2$, and $ZnBr_2$) in the presence of base by high resolution mass spectrometry. Again, we observed species that were consistent with the formation of **M$_3$Br$_6$·^{OPr}cage′** complexes (see Supporting Information Section 6). However, when we studied the coordination of $ZnBr_2$ to ^{OPr}**cage′** using NMR spectroscopy, it became apparent that the nature of the **Zn$_3$Br$_6$·^{OPr}cage′** complex was very different from that of **Zn$_3$Br$_6$·^{Et}cage′**. The room temperature ^{1}H NMR spectrum of ^{OPr}**cage′** in the presence of base and 3.0 equivalents of $ZnBr_2$ in DMSO-d$_6$ (Figure 3a) gave a significantly more complex and broad spectrum than had been observed using the ethyl-substituted cage (Figure 2a). To investigate this further, we prepared and isolated **Zn$_3$Br$_6$·^{OPr}cage′** in 87% yield and characterised it by 1D and 2D NMR techniques and high resolution mass spectrometry (see Supporting Information Section 1 for full details).

We first conducted VT-^{1}H NMR studies on **Zn$_3$Br$_6$·^{OPr}cage′**, and found that heating caused the broad spectrum to sharpen considerably. At 360 K (Figure 3a), a sharp, well-resolved spectrum was obtained with two sets of peaks for all downfield resonances in a 2:1 ratio, suggesting that two arms of the cage are in a different environment to

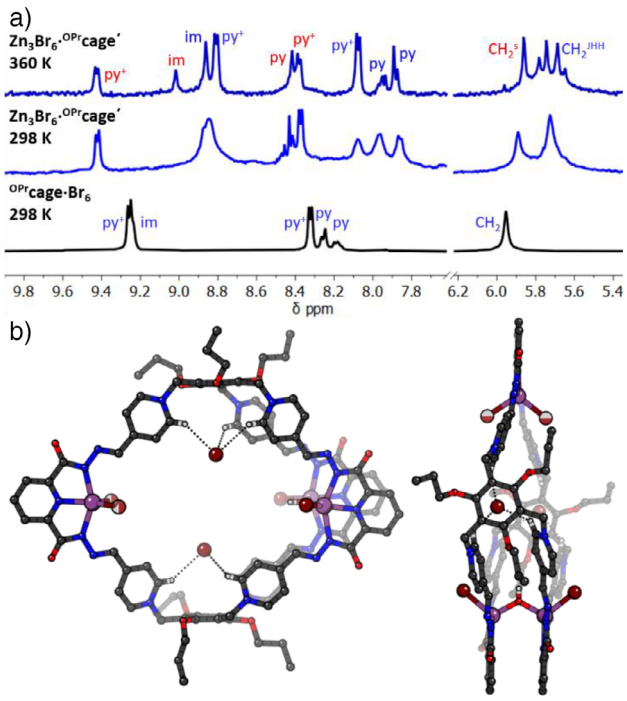

Figure 3. Complexation of $ZnBr_2$ to ^{OPr}**cage·Br$_6$**: a) partial ^{1}H NMR spectra of ^{OPr}**cage·Br$_6$** at 298 K (black spectrum), **Zn$_3$Br$_6$·^{OPr}cage′** at 298 K (blue spectrum) and **Zn$_3$Br$_6$·^{OPr}cage′** at 360 K (navy spectrum) (2.0 mM in DMSO-d$_6$, 400 MHz); b) two views of the X-ray crystal structure of **Zn$_3$Br$_5$(μ-OH)·^{OPr}cage′** (dotted lines indicate H-bonding interactions shorter than the sum of the van der Waals radii[61] of H and Br), PLATON-SQUEEZE[62] was used to remove ill-defined solvent molecules in the cage cavity.

the third. 2D NOESY and TOCSY experiments conducted at 360 K confirmed this assignment and further indicated that the two equivalent cage arms are close to one another in space. Consistent with this inequivalency, the single methylene CH_2 resonance in the free cage is present as two peaks in $\mathbf{Zn_3Br_6}\cdot{}^{\mathbf{OPr}}\mathbf{cage'}$: a singlet due to the isolated arm of the cage and a diastereotopic AB quartet resulting from geminal coupling between the inequivalent protons on the two close in-space cage arms. Further evidence for the proposed structure of $\mathbf{Zn_3Br_6}\cdot{}^{\mathbf{OPr}}\mathbf{cage'}$ was provided by $^{13}C\{^1H\}$ NMR spectroscopy, which revealed a doubling of resonances compared to the uncomplexed cage, and DOSY NMR spectroscopy which showed that all peaks in the ^1H NMR spectrum belonged to a single species (calculated solvodynamic radius = 15.5 Å, within 5% of that of the uncomplexed cage).

The conformation of this cage complex was determined unambiguously by X-ray crystallography (Figure 3b), which confirmed the assignments made by NMR spectroscopy. Two arms of the cage are located close to one another, while the other is located far away, giving $^{\mathbf{OPr}}\mathbf{cage'}$ a much flatter structure than observed in the metal complexes of $^{\mathbf{Et}}\mathbf{cage'}$. The two adjacent zinc(II) ions are bridged by a hydroxide group, i.e., in the crystal the cage has the formula $\mathbf{Zn_3Br_5(\mu\text{-}OH)}\cdot{}^{\mathbf{OPr}}\mathbf{cage'}$ (Zn···Zn distance = 3.414(1) Å, Zn···O distances = 1.936(5) and 1.941(5) Å, entirely consistent with that expected for a Zn(II)–hydroxide bond based on analysis of the CSD,[60] see Supporting Information Section 9).[63] The zinc(II) ions again have geometries intermediate between square pyramidal and trigonal bipyramidal (τ_5 = 0.31–0.35). Again, there are two bromide anions located in the tris-pyridinium pockets provided by the cage caps, and the two hydroxide-bridged zinc(II) ions each coordinate to one bromide anion in addition to three N-donors from the pincer and the hydroxide group. The third zinc(II) binds to two half-occupancy bromide anions (presumably a solvent is coordinated when the half-occupancy bromides are absent, but this could not be resolved crystallographically).

Low Symmetry Complexes of ^{OPr}Cage′ Form With Several Different Anions

We find it remarkable that the low symmetry cage arrangement occurs at temperatures as high as 360 K and were intrigued to discover if it was specific to the Br^- salt of the Zn(II) complex. To this end, we prepared and isolated $\mathbf{Zn_3(OAc)_6}\cdot{}^{\mathbf{OPr}}\mathbf{cage'}$ through an anion exchange reaction and studied this complex using 1D and 2D NMR spectroscopies, high resolution ESI mass spectrometry and X-ray crystallography. Solution NMR studies again showed a low symmetry species with two sets of peaks that integrated to a 2:1 ratio, and the X-ray crystal structure has two arms of the cage close together bridged by an acetate ligand. Interestingly, this pushes the two "close" arms further apart from one another than in the Br^- complex (Figure S144, Zn···Zn distance = 6.03(2) Å) to accommodate the larger κ^2-*O,O′* bridging mode of the OAc^- ligand, demonstrating that this low symmetry arrangement can adapt to bridging ligands of quite different sizes. Further studies were conducted by preparing the $ZnCl_2$, ZnI_2, and $Zn(OTf)_2$ complexes of $^{\mathbf{OPr}}\mathbf{cage'}$; in all cases these had NMR spectra consistent with low symmetry complexes (Figures S67, S69, and S72).

While the focus of the current work is on cage synthesis and structure, we were interested to see if the bridged low symmetry metallocages displayed different functionality to the high symmetry cage complexes. We conducted preliminary studies of guest binding to $\mathbf{Zn_3Br_6}\cdot{}^{\mathbf{Et}}\mathbf{cage'}$ and $\mathbf{Zn_3Br_6}\cdot{}^{\mathbf{OPr}}\mathbf{cage'}$ in DMSO-d_6 (used for solubility reasons). Addition of SO_4^{2-} to high symmetry non-bridged $\mathbf{Zn_3Br_6}\cdot{}^{\mathbf{Et}}\mathbf{cage'}$ resulted in minimal changes to the ^1H NMR spectrum, suggesting negligible binding (Figure S94).[64] In contrast, addition of SO_4^{2-} to low symmetry $\mathbf{Zn_3Br_6}\cdot{}^{\mathbf{OPr}}\mathbf{cage'}$ results in quantitative formation of a new low symmetry species in slow exchange with $\mathbf{Zn_3Br_6}\cdot{}^{\mathbf{OPr}}\mathbf{cage'}$ (Figure S88). While we have not yet been able to conclusively identify the binding mode, we suggest the strong sulfate binding arises from the preorganisation of two Zn^{2+} centres in close proximity that can then coordinate to the anion (HRESI-MS is also consistent with formation of a metalated cage species bound to a single SO_4^{2-} anion, Figure S93). Clearly, the low symmetry arrangement of the cage results in a dramatic change in guest binding properties.

Synthesis of ^{OMe}cage·Br_6 and ^{H}cage·Br_6 and Their Low Symmetry Complexes

To further investigate the effect of R-groups on cage conformation, we next prepared $^{\mathbf{H}}\mathbf{cage}\cdot\mathbf{Br_6}$ and $^{\mathbf{OMe}}\mathbf{cage}\cdot\mathbf{Br_6}$ containing either no R-groups (i.e., R=H) or methoxy substituents, respectively. These cages were prepared in a single step from the corresponding tris-pyridinium tripods and 2,6-pyridinedicarbohydrazide in 77% ($^{\mathbf{H}}\mathbf{cage}\cdot\mathbf{Br_6}$) and 67% ($^{\mathbf{OMe}}\mathbf{cage}\cdot\mathbf{Br_6}$) yields and isolated by simple precipitation and filtration. The new cages were characterised by ^1H, $^{13}C\{^1H\}$ and DOSY NMR spectroscopy as well as high resolution mass spectrometry (see Supporting Information Section 1).

The cages were metalated with $ZnBr_2$ in the presence of NEt_3 in DMSO-d_6 to give $\mathbf{Zn_3Br_6}\cdot{}^{\mathbf{H}}\mathbf{cage'}$ and $\mathbf{Zn_3Br_6}\cdot{}^{\mathbf{OMe}}\mathbf{cage'}$. The methoxy-substituted complex adopts a low symmetry complex, with a very similar ^1H NMR spectrum to that of $\mathbf{Zn_3Br_6}\cdot{}^{\mathbf{OPr}}\mathbf{cage'}$, and this low symmetry arrangement persists even at elevated temperatures (Figures S85 and S87). Interestingly, $\mathbf{Zn_3Br_6}\cdot{}^{\mathbf{H}}\mathbf{cage'}$ gives a high symmetry ^1H NMR spectrum in DMSO-d_6 (Figure S81), but takes on a low symmetry arrangement in 1:1 DMSO-d_6:D_2O (Figure S84). The low symmetry arrangement persists in this mixed solvent even at elevated temperature. It appears that the R=H cage exists in a middle ground where neither the high symmetry or low symmetry arrangement is dramatically preferred and so solvent can be used to switch conformation.

Pd(II) Complexes of ^{Et}Cage′ and ^{OPr}Cage′ Show Distinct Conformations

We next studied another diamagnetic metal ion, Pd(II). The square planar geometry of this ion makes bridged complexes

unlikely so we were intrigued to see how Pd(II) complexes of ^{Et}**cage**′ and ^{OPr}**cage**′ compared with the Zn(II) complexes. Complexation with $[PdBr_2(NCCH_3)_2]$ in DMSO-d_6 in the presence of NEt_3 gave species with only one set of NMR signals in both cases, suggesting time-averaged symmetry in solution. X-ray crystal structures show that **Pd$_3$Br$_6$**·^{Et}**cage**′ adopts a structure with the three arms distant from one another, while in the solid state **Pd$_3$Br$_6$**·^{OPr}**cage**′ takes on a flattened structure with two arms close together (Figure 4). In this structure the arms are not held together by any bridging ligands, as expected for square planar Pd. However, the Pd(II) ions are closer than the sum of their van der Waals radii[61] (Pd···Pd distance = 3.652(1) Å, 85% of the sum of the van der Waals radii) suggesting a potentially favourable metallophilic interaction in the solid state, although we note that these type of interactions are vanishingly weak in solution.[65] Interestingly, similarly short Pd···Pd contacts are observed in the crystal structure of **Pd$_3$Br$_6$**·^{Et}**cage**′ but in this case, these interactions occur between adjacent cage molecules (Figure S136).

While the ^{1}H NMR spectrum of **Pd$_3$Br$_6$**·^{OPr}**cage**′ has three-fold symmetry, there are relatively significant differences between the NMR spectra of **Pd$_3$Br$_6$**·^{Et}**cage**′ and **Pd$_3$Br$_6$**·^{OPr}**cage**′ (Figure S100), and indeed between the NMR spectra of ^{Et}**cage**·**Br$_6$** and ^{OPr}**cage**·**Br$_6$** (Figure S98). In both cases, peaks far from the solubilising groups such as the external pyridyl resonances and imine groups occur at values 0.1–0.2 ppm lower in the propoxy-substituted cage than the ethyl-substituted cage. These lower ppm values are consistent with aromatic stacking arrangements between cage arms occurring to some extent. We attempted to conduct low temperature NMR studies to see if the cage arms became inequivalent upon cooling, but unfortunately we were hampered by precipitation at these temperatures. Attempts to see if adding water to the solvent mixture favoured a low symmetry conformation were also hampered by precipitation. Given the differences between the NMR spectra of the different cages, as well as the low symmetry single crystal structure of **Pd$_3$Br$_6$**·^{OPr}**cage**′, we think it is reasonable to speculate that both ^{OPr}**cage**·**Br$_6$** and **Pd$_3$Br$_6$**·^{OPr}**cage**′ are dynamic in solution, and that part of the time two arms come close together, presumably driven by favourable solvophobic stacking interactions. We do not see evidence of this in the ethyl-substituted cage, presumably due to the steric clashes this would cause with the ethyl substituent (see later).

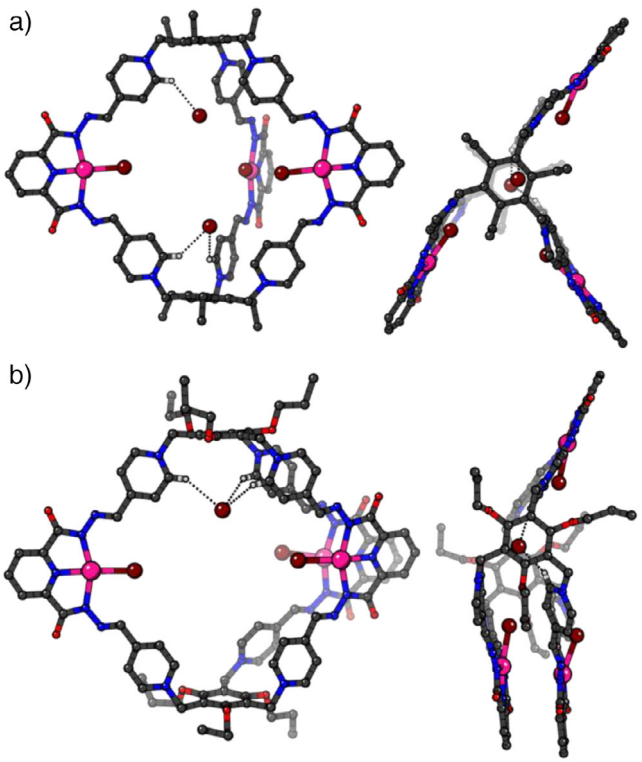

Figure 4. X-ray crystal structures of a) **Pd$_3$Br$_6$**·^{Et}**cage**′ and b) **Pd$_3$Br$_6$**·^{OPr}**cage**′, PLATON-SQUEEZE[62] was used to remove ill-defined solvent molecules in the cage cavity.

Why Does Changing a Solubilising Group Change Cage Conformation?

It is remarkable that the apparently trivial change from ethyl substituents to alkoxy substituents on the cap groups of the cages should have such a dramatic effect on the conformation of the resulting metallocage. We hypothesised that this was likely due to interactions between these substituents and the cage arms (Figure 5a). Bringing two cage arms close together to reach the low symmetry flattened arrangement requires the first atom of the cage arm (a CH_2 group bonded to a pyridinium nitrogen atom) to be close in space to the first atom of the ethyl/alkoxy group. In the ethyl group, this is a CH_2 group, while in the alkoxy group this

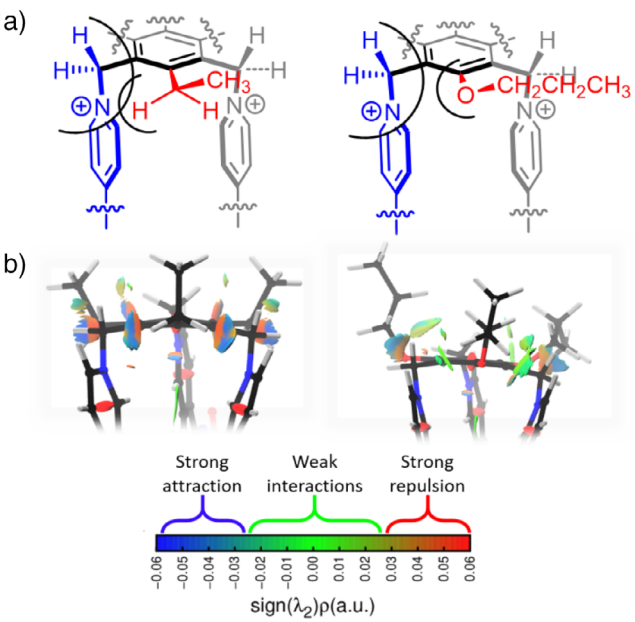

Figure 5. a) Partial structure of ^{R}**cage**′ indicating the close proximity of the Et/OPr groups to the pyridinium CH_2 groups; b) NCI isosurface analysis of the r^{2}SCAN-3c[69,70]-optimised structures of **Zn$_3$Br$_5$(μ-OH)**·^{OPr}**cage**′ and **Zn$_3$Br$_5$(μ-OH)**·^{Et}**cage**′ showing attractive (blue), weak (green), and repulsive (red) interactions.

is a slightly smaller oxygen atom, which may reduce steric repulsion and be able to form weak attractive interactions with the electron deficient pyridinium–CH_2 hydrogen atoms. To study this, the total energies, exchange energies (proxy for sterics and indicator of Pauli repulsion[66]) and dispersion energies of homodesmotic "couples"[67,68] of DFT (r^{2}SCAN-3c[69,70]) optimised structures of $\mathbf{Zn_3Br_5(\mu\text{-}OH)\cdot{}^{OPr}cage'}$ and $\mathbf{Zn_3Br_5(\mu\text{-}OH)\cdot{}^{Et}cage'}$, i.e., the structure that would result if $\mathbf{^{Et}cage'}$ took on the low symmetry flattened structure with a bridging hydroxide ligand, were compared. Interestingly, we found that $\mathbf{Zn_3Br_5(\mu\text{-}OH)\cdot{}^{OPr}cage'}$ is indeed more energetically favourable than $\mathbf{Zn_3Br_5(\mu\text{-}OH)\cdot{}^{Et}cage'}$ by 12 kJ mol^{-1}, with the propoxy-based metallocage experiencing less apparent steric repulsion[66] and more favourable dispersion energy (see Supporting Information Section 10 for further analysis). This can be visually observed using computational non-covalent interaction (NCI[71]) analysis. As shown in Figure 5b, for both $\mathbf{Zn_3Br_5\mu\text{-}OH\cdot{}^{OPr}cage'}$ and $\mathbf{Zn_3Br_5\mu\text{-}OH\cdot{}^{Et}cage'}$ there are NCI densities between the solubilising groups and the pyridinium–CH_2 hydrogen atoms. In the case of $\mathbf{^{Et}cage'}$ (Figure 5b left), these associations are weakly repulsive while for $\mathbf{^{OPr}cage'}$ there appear to be more dispersion interactions (Figure 5b right). In light of these theoretical analyses, we suggest that the presence of other favourable interactions such as coordination to bridging ligands in the zinc(II) complexes, or solvophobic stacking interactions between the planar cage arms can overcome relatively low repulsive steric costs in the case of $\mathbf{^{OPr}cage'}$. In contrast, the additional repulsion in the case of $\mathbf{^{Et}cage'}$ means that this is far harder to do. Computational analysis of $\mathbf{^{H}cage'}$ suggests little energy difference between the bridged and nonbridged conformations, consistent with the experimental observations that this cage has a high symmetry nonbridged arrangement in DMSO-d_6, but a bridged low symmetry arrangement in 1:1 D_2O:DMSO-d_6.

Conclusion

In this work, we have reported what we believe to be a new approach to persistently low symmetry metal organic cages, where an organic cage is metalated and this metal ion induces a loss of symmetry between otherwise identical cage arms. Depending on the substituent located between the cage arms and the metal ions, very different behaviour is observed. Zn(II) complexes of $\mathbf{^{Et}cage'}$ have the expected three-fold symmetry, while Zn(II) complexes of $\mathbf{^{OMe}cage'}$ and $\mathbf{^{OPr}cage'}$ have a low symmetry arrangement, with two arms distinct from the third. Remarkably this low symmetry arrangement persists even at elevated temperatures (360 K), and in the presence of a range of anions. Zn(II) complexes of $\mathbf{^{H}cage'}$ preferentially adopt a high symmetry arrangement in DMSO, but a low symmetry conformation in DMSO/water mixtures. We believe that this represents a new and likely generalisable way to prepare low symmetry metal cages. Furthermore, we think that these metallocages containing metal ions pointing towards a central cage cavity may be interesting systems to study for enzyme-inspired catalysis, and work investigating this is underway in our laboratories.

Experimental Section

Synthetic procedures, characterisation data, metal binding studies, details of X-ray crystallography and computational chemistry are provided in the Supporting Information.

Supporting Information

The authors have cited additional references within the Supporting Information.[72–89]

Acknowledgements

The authors thank the Australian Research Council for funding (DP230100190 to ALC and NGW). Parts of this work were conducted using the MX2 beamline[80] at the Australian Synchrotron, part of ANSTO, and made use of the Australian Cancer Research Foundation (ACRF) detector. This research was undertaken with the assistance of resources from the National Computational Infrastructure (NCI Australia), and NCRIS enabled capability supported by the Australian Government. The authors thank Gareth Nelmes and Dr Dan Preston for useful discussions.

Open access publishing facilitated by Australian National University, as part of the Wiley - Australian National University agreement via the Council of Australian University Librarians.

Conflict of Interests

The authors declare no conflict of interest.

Data Availability Statement

The data that support the findings of this study are available in the supplementary material of this article.

Deposition Numbers 2463022 (for $\mathbf{Pd_3Br_6\cdot{}^{Et}cage'}$), 2463023 (for $\mathbf{Zn_3Br_6\cdot{}^{Et}cage'}$), 2463024 (for $\mathbf{Zn_3(OAc)_6\cdot{}^{Et}cage'}$), 2463025 (for $\mathbf{Zn_3Br_6\cdot{}^{Et}cage'}$), 2463026 (for $\mathbf{Zn_3(OAc)_6\cdot{}^{OPr}cage'}$), 2463027 (for $\mathbf{Cu_3Br_6\cdot{}^{Et}cage'}$), 2463028 (for $\mathbf{Pd_3Br_6\cdot{}^{OPr}cage'}$) and 2463029 (for $\mathbf{Zn_3Br_6\cdot{}^{OPr}cage'}$) contain the supplementary crystallographic data for this paper. These data are provided free of charge by the joint Cambridge Crystallographic Data Centre and Fachinformationszentrum Karlsruhe Access Structures service.

Keywords: Cages · Low symmetry · Metallocages · R groups · Supramolecular chemistry

[1] T. K. Piskorz, V. Martí-Centelles, R. L. Spicer, F. Duarte, P. J. Lusby, *Chem. Sci.* **2023**, *14*, 11300–11331.
[2] W. M. Bloch, G. H. Clever, *Chem. Commun.* **2017**, *53*, 8506–8516.
[3] C. T. McTernan, J. A. Davies, J. R. Nitschke, *Chem. Rev.* **2022**, *122*, 10393–10437.
[4] J. E. M. Lewis, *Chem. Commun.* **2022**, *58*, 13873–13886.
[5] A. M. Johnson, R. J. Hooley, *Inorg. Chem.* **2011**, *50*, 4671–4673.
[6] D. Preston, J. E. Barnsley, K. C. Gordon, J. D. Crowley, *J. Am. Chem. Soc.* **2016**, *138*, 10578–10585.
[7] J. Tessarolo, H. Lee, E. Sakuda, K. Umakoshi, G. H. Clever, *J. Am. Chem. Soc.* **2021**, *143*, 6339–6344.
[8] M. Schmittel, B. He, *Chem. Commun.* **2008**, 4723 10.1039/b808988d.
[9] J.-R. Li, H.-C. Zhou, *Nat. Chem.* **2010**, *2*, 893–898.
[10] Y.-R. Zheng, Z. Zhao, M. Wang, K. Ghosh, J. B. Pollock, T. R. Cook, P. J. Stang, *J. Am. Chem. Soc.* **2010**, *132*, 16873–16882.
[11] Q.-F. Sun, S. Sato, M. Fujita, *Angew. Chem. Int. Ed.* **2014**, *53*, 13510–13513.
[12] W. M. Bloch, Y. Abe, J. J. Holstein, C. M. Wandtke, B. Dittrich, G. H. Clever, *J. Am. Chem. Soc.* **2016**, *138*, 13750–13755.
[13] S. Prusty, K. Yazaki, M. Yoshizawa, D. K. Chand, *Chem. – Eur. J.* **2017**, *23*, 12456–12461.
[14] D. Ogata, J. Yuasa, *Angew. Chem. Int. Ed.* **2019**, *58*, 18424–18428.
[15] J. E. M. Lewis, A. Tarzia, A. J. P. White, K. E. Jelfs, *Chem. Sci.* **2020**, *11*, 677–683.
[16] S. Sudan, R.-J. Li, S. M. Jansze, A. Platzek, R. Rudolf, G. H. Clever, F. Fadaei-Tirani, R. Scopelliti, K. Severin, *J. Am. Chem. Soc.* **2021**, *143*, 1773–1778.
[17] J. E. M. Lewis, *Angew. Chem. Int. Ed.* **2022**, *61*, e202212392.
[18] M. Parbin, V. Sivalingam, D. K. Chand, *Angew. Chem. Int. Ed.* **2024**, *63*, e202410219.
[19] J. A. Gome, Z. T. Avery, N. R. Lawson, O. G. Stansfield, J. D. Evans, M. G. Gardiner, T. U. Connell, D. Preston, *Angew. Chem. Int. Ed.* **2025**, *64*, e202503473.
[20] D. Preston, J. D. Evans, *Angew. Chem. Int. Ed.* **2023**, *62*, e202314378.
[21] T. Abe, N. Sanada, K. Takeuchi, A. Okazawa, S. Hiraoka, *J. Am. Chem. Soc.* **2023**, *145*, 28061–28074.
[22] K. Wu, E. Benchimol, A. Baksi, G. H. Clever, *Nat. Chem.* **2024**, *16*, 584–591.
[23] E. Berardo, R. L. Greenaway, L. Turcani, B. M. Alston, M. J. Bennison, M. Miklitz, R. Clowes, M. E. Briggs, A. I. Cooper, K. E. Jelfs, *Nanoscale* **2018**, *10*, 22381–22388.
[24] R. L. Greenaway, V. Santolini, F. T. Szczypiński, M. J. Bennison, M. A. Little, A. Marsh, K. E. Jelfs, A. I. Cooper, *Chem. – Eur. J.* **2020**, *26*, 3718–3722.
[25] V. Abet, F. T. Szczypiński, M. A. Little, V. Santolini, C. D. Jones, R. Evans, C. Wilson, X. Wu, M. F. Thorne, M. J. Bennison, P. Cui, A. I. Cooper, K. E. Jelfs, A. G. Slater, *Angew. Chem. Int. Ed.* **2020**, *59*, 16755–16763.
[26] M. Otte, M. Lutz, R. J. M. Klein Gebbink, *Eur. J. Org. Chem.* **2017**, *2017*, 1657–1661.
[27] S. C. Bete, L. K. May, P. Woite, M. Roemelt, M. Otte, *Angew. Chem. Int. Ed.* **2022**, *61*, e202206120.
[28] K. G. Andrews, P. N. Horton, S. J. Coles, *Chem. Sci.* **2024**, *15*, 6536–6543.
[29] A. Burgun, P. Valente, J. D. Evans, D. M. Huang, C. J. Sumby, C. J. Doonan, *Chem. Commun.* **2016**, *52*, 8850–8853.
[30] A.-D. Manick, J.-P. Dutasta, A. Martinez, *ChemPlusChem* **2023**, *88*, e202300291.
[31] C. M. Thomas, N. G. White, *Supramol. Chem.* **2023**, *34*, 326–338.
[32] J.-X. Wang, S.-C. Li, L.-X. Cai, S.-J. Hu, L.-P. Zhou, J. Yang, Q.-F. Sun, *Org. Lett.* **2024**, *26*, 4152–4157.
[33] Shortly before submission of this manuscript, Prof. Hao Li (Zhejiang University) presented unpublished results at the 2025 ISMSC conference describing a hexa-cationic organic cage that adopts a low symmetry conformation in the absence of a coordinating anion, but becomes higher symmetry upon anion coordination. While not directly related, we note that this in some ways represents the "inverse" of the results reported here.
[34] V. Steinmetz, F. Couty, O. R. P. David, *Chem. Commun.* **2009**, 343–345. 10.1039/B816628E.
[35] Y. Makita, K. Sugimoto, K. Furuyoshi, K. Ikeda, S. Fujiwara, T. Shin-ike, A. Ogawa, *Inorg. Chem.* **2010**, *49*, 7220–7222.
[36] G. L. Guillet, F. T. Sloane, M. F. Dumont, K. A. Abboud, L. J. Murray, *Dalton Trans.* **2012**, *41*, 7866.
[37] G. L. Guillet, F. T. Sloane, D. M. Ermert, M. W. Calkins, M. K. Peprah, E. S. Knowles, E. Čižmár, K. A. Abboud, M. W. Meisel, L. J. Murray, *Chem. Commun.* **2013**, *49*, 6635.
[38] L. J. Murray, W. W. Weare, J. Shearer, A. D. Mitchell, K. A. Abboud, *J. Am. Chem. Soc.* **2014**, *136*, 13502–13505.
[39] P. T. Smith, B. P. Benke, Z. Cao, Y. Kim, E. M. Nichols, K. Kim, C. J. Chang, *Angew. Chem. Int. Ed.* **2018**, *57*, 9684–9688.
[40] H. Wang, Y. Jin, N. Sun, W. Zhang, J. Jiang, *Chem. Soc. Rev.* **2021**, *50*, 8874–8886.
[41] M. M. Deegan, R. Bhattacharjee, S. Caratzoulas, E. D. Bloch, *Inorg. Chem.* **2021**, *60*, 7044–7050.
[42] C. M. Thomas, W. Liang, D. Preston, C. J. Doonan, N. G. White, *Chem. – Eur. J.* **2022**, *28*, e202200958.
[43] É. M. Foyle, R. J. Goodwin, C. J. T. Cox, B. R. Smith, A. L. Colebatch, N. G. White, *J. Am. Chem. Soc.* **2024**, *146*, 27127–27137.
[44] M. Nonoyama, *Inorganica Chim. Acta* **1974**, *10*, 59–63.
[45] S. K. Sahni, S. K. Sangal, S. P. Gupta, V. B. Rana, *J. Inorg. Nucl. Chem.* **1977**, *39*, 1098–1100.
[46] A. K. Patra, R. Mukherjee, *Inorg. Chem.* **1999**, *38*, 1388–1393.
[47] D. Huang, R. H. Holm, *J. Am. Chem. Soc.* **2010**, *132*, 4693–4701.
[48] P. J. Donoghue, J. Tehranchi, C. J. Cramer, R. Sarangi, E. I. Solomon, W. B. Tolman, *J. Am. Chem. Soc.* **2011**, *133*, 17602–17605.
[49] P. Pirovano, E. R. Farquhar, M. Swart, A. J. Fitzpatrick, G. G. Morgan, A. R. McDonald, *Chem. – Eur. J.* **2015**, *21*, 3785–3790.
[50] T. Corona, F. F. Pfaff, F. Acuña-Parés, A. Draksharapu, C. J. Whiteoak, V. Martin-Diaconescu, J. Lloret-Fillol, W. R. Browne, K. Ray, A. Company, *Chem. – Eur. J.* **2015**, *21*, 15029–15038.
[51] Y. M. Kwon, Y. Lee, G. E. Evenson, T. A. Jackson, D. Wang, *J. Am. Chem. Soc.* **2020**, *142*, 13435–13441.
[52] D. Prabha, D. Singh, P. Kumar, R. Gupta, *Inorg. Chem.* **2021**, *60*, 17889–17899.
[53] While we are not aware of any reports where changing R-substituents leads to changes in cage symmetry, adding alkyl substituents to similar tri-substituted benzene rings has been seen to have a small effect in supramolecular host-guest chemistry,[54] and to have relatively large effects on catalysis.[55].
[54] X. Wang, F. Hof, *Beilstein J. Org. Chem.* **2012**, *8*, 1–10.
[55] D. H. Hong, R. B. Ferreira, V. J. Catalano, R. García-Serres, J. Shearer, L. J. Murray, *Inorg. Chem.* **2021**, *60*, 7228–7239.
[56] J. C. Lauer, A. S. Bhat, C. Barwig, N. Fritz, T. Kirschbaum, F. Rominger, M. Mastalerz, *Chem. – Eur. J.* **2022**, *28*, e202201527.
[57] We used the bromide salts of these metals and the bromide salt of the cage to avoid formation of mixed salts.
[58] These complexes tend to contain mixtures of coordinated and non-coordinated anions and coordinated solvent molecules, so in the interest of simplicity we use this general naming rather than typical coordination complex formulae.
[59] A. W. Addison, T. N. Rao, J. Reedijk, J. van Rijn, G. C. Verschoor, *J. Chem. Soc., Dalton Trans.* **1984**, 1349–1356. 10.1039/DT9840001349.
[60] R. Taylor, P. A. Wood, *Chem. Rev.* **2019**, *119*, 9427–9477.
[61] S. Alvarez, *Dalton Trans.* **2013**, *42*, 8617.

[62] A. L. Spek, *Acta Crystallogr.* **2015**, *C71*, 9–18.
[63] A reviewer questioned whether the low symmetry coordination arrangement may be due to the presence of hydroxide. This does not seem to be the case, as adding small amounts of hydroxide to either $\mathbf{Zn_3Br_6}\cdot{}^{\mathbf{Et}}\mathbf{cage'}$ or $\mathbf{Zn_3Br_6}\cdot{}^{\mathbf{OPr}}\mathbf{cage'}$ does not cause a change in their NMR spectra (Figure S96 and S97). Adding large amounts of hydroxide leads to decomposition and precipitation. The hydroxide in this crystal structure presumably results from deprotonation of adventitious water, facilitated by the proximity of two Zn^{2+} centres.
[64] We note that uncomplexed $^{\mathbf{Et}}\mathbf{cage}\cdot\mathbf{Br_6}$ displays moderate sulfate binding in DMSO/water mixtures.[43] It appears that removing the amide N–H groups due to complexation of zinc(II) "turns off" this sulfate binding ability for $^{\mathbf{Et}}\mathbf{cage'}$.
[65] Q. Zheng, S. Borsley, G. S. Nichol, F. Duarte, S. L. Cockroft, *Angew. Chem. Int. Ed.* **2019**, *58*, 12617–12623.
[66] M. Bursch, S. Grimme, A. Hansen, *Acc. Chem. Res.* **2024**, *57*, 153–163.
[67] P. George, M. Trachtman, C. W. Bock, A. M. Brett, *Theor. Chim Acta* **1975**, *38*, 121–129.
[68] P. George, M. Trachtman, C. W. Bock, A. M. Brett, *J. Chem. Soc., Perkin Trans.* **1976**, *2*, 1222.
[69] S. Grimme, A. Hansen, S. Ehlert, J.-M. Mewes, *J. Chem. Phys.* **2021**, *154*, 064103.
[70] M. Bursch, J.-M. Mewes, A. Hansen, S. Grimme, *Angew. Chem. Int. Ed.* **2022**, *61*, e202205735.
[71] J. Contreras-García, E. R. Johnson, S. Keinan, R. Chaudret, J.-P. Piquemal, D. N. Beratan, W. Yang, *J. Chem. Theory Comput.* **2011**, *7*, 625–632.
[72] H. E. Gottlieb, V. Kotlyar, A. Nudelman, *J. Org. Chem.* **1997**, *62*, 7512–7515.
[73] *MNova 14.2*, MestreLab Research, **2022**.
[74] B. R. Cho, K. Chajara, H. J. Oh, K. H. Son, S.-J. Jeon, *Org. Lett.* **2002**, *4*, 1703–1706.
[75] D. Wang, S. Mirzaei, S. V. Lindeman, R. Rathore, *Tetrahedron Lett.* **2019**, *60*, 151215.
[76] R. M. Duke, J. E. O'Brien, T. Mccabe, T. Gunnlaugsson, *Org. Biomol. Chem.* **2008**, *6*, 4089.
[77] D. C. Ebner, R. M. Trend, C. Genet, M. J. Mcgrath, P. O'Brien, B. M. Stoltz, *Angew. Chem. Int. Ed.* **2008**, *47*, 6367–6370.
[78] M. Christensen, M. Rimmen, M. Nielsen, *Synlett* **2013**, *24*, 2715–2719.
[79] M. D. Carmen Grande, J. A. Juliá, M. García, C. M. Marschoff, *J. Chem. Thermodyn.* **2007**, *39*, 1049–1056.
[80] D. Aragão, J. Aishima, H. Cherukuvada, R. Clarken, M. Clift, N. P. Cowieson, D. J. Ericsson, C. L. Gee, S. Macedo, N. Mudie, S. Panjikar, J. R. Price, A. Riboldi-Tunnicliffe, R. Rostan, R. Williamson, T. T. Caradoc-Davies, *J. Synchrotron Radiat.* **2018**, *25*, 885–891.
[81] W. Kabsch, *Acta Crystallogr.* **2010**, *D66*, 125–132.
[82] G. Sheldrick, *Acta Crystallogr.* **2015**, *A71*, 3–8.
[83] P. W. Betteridge, J. R. Carruthers, R. I. Cooper, K. Prout, D. J. Watkin, *J. Appl. Crystallogr.* **2003**, *36*, 1487.
[84] *CrysAlis Pro, Oxford Diffraction*, **2011**.
[85] *Spartan24*, Wavefunction Inc. **2025**.
[86] F. Neese, *WIREs Comput. Mol. Sci.* **2022**, *12*, e1606.
[87] F. Weigend, R. Ahlrichs, *Phys. Chem. Chem. Phys.* **2005**, *7*, 3297.
[88] T. Novoa, R. Laplaza, F. Peccati, F. Fuster, J. Contreras-García, *J. Chem. Inf. Model.* **2023**, *63*, 4483–4489.
[89] W. Humphrey, A. Dalke, K. Schulten, *J. Mol. Graph.* **1996**, *14*, 33–38.

Manuscript received: June 16, 2025
Revised manuscript received: July 29, 2025
Accepted manuscript online: August 06, 2025
Version of record online: ■■, ■■